JOURNAL OF MATERIALS SCIENCE **34** (1999) 3567–3575

An investigation of the fatigue and fracture behavior of multicomponent Nb-11Al-41Ti-1.5Mo-1.5Cr intermetallic

W. O. SOBOYEJO, F. YE, J. DIPASQUALE
Department of Materials Science and Engineering, The Ohio State University, 116 West 19th Avenue, Columbus, OH 43210, USA

P. PINE
Department of Materials Science and Engineering, MIT, 77 Massachusetts Avenue, Cambridge, MA 02139, USA

This paper presents the results of a recent study of the fracture and fatigue crack growth behavior of a newly developed multicomponent niobium aluminide intermetallic Nb-11Al-41Ti-1.5Mo-1.5Cr alloy (compositions quoted in at% unless stated otherwise). The alloy is shown to have attractive combinations of room-temperature tensile ductility (approx. 11%) and fracture toughness (approx. 83 MPa$\sqrt{\text{m}}$) in the as-forged condition. However, the tensile properties and fracture toughness are degraded somewhat by direct aging at 750 °C for 25 h. The direct aged Nb-11Al-41Ti-1.5Mo-1.5Cr intermetallic is also shown to have comparable fatigue crack growth resistance to pure Nb, IN 718 and mill annealed Ti-6Al-4V at room- and elevated-temperature. Fatigue and fracture mechanisms are elucidated prior to a discussion of the implications of the current results for potential high temperature structural applications.

1. Introduction

Niobium aluminide-based intermetallics are being considered as potential structural materials for applications in the 700 to 800 °C temperature regime [1]. The interest in this new class of B2 + orthorhombic intermetallics is due to their moderate densities (∼6.1 g/cm^3), room-temperature fracture toughness (∼40–100 MPa$\sqrt{\text{m}}$) [2, 3] and fatigue resistance [2–5]. The niobium aluminide intermetallics also have attractive combinations of room temperature ductility (approx. 3–30%) [1–4] and strength retention at temperature up to approx. 700 °C.

However, the isothermal and cyclic oxidation resistance of the niobium aluminide based alloys determine the limits to their use at elevated temperature [6, 7]. Previous work by Li *et al.* [6] has shown that niobium aluminide (Nb_3Al-xTi) alloys have sufficient oxidation resistance for use as uncoated structural materials in the temperature regime below 750 °C. Mixed oxides, consisting of complex mixtures of TiO_2, Nb_2O_5 and Al_2O_3 have also been observed to form during the isothermal oxidation of Nb_3Al-xTi ($x = 10$–40 at%) alloys.

Prior work on niobium aluminide intermetallics has demonstrated that alloying with chromium can increase the potential service conditions by ∼50 °C from 750 to ∼800 °C [7]. However, levels of Cr > 5% also resulted in the complete loss of room-temperature ductility, which is one of the attractive features of this new class of alloys [7]. Furthermore, alloying of niobium aluminide alloys with 1.5Mo has also been shown to increase the creep rupture lives of niobium aluminide alloys. Prior work therefore suggests that an alloy with a balance of creep and oxidation resistance may be engineered in niobium aluminide intermetallics by alloying with Cr and Mo.

The current paper presents the results of a recent study of the fatigue and fracture behavior of a niobium aluminide alloy in which 1.5Mo and 1.5Cr have been added for the improvement of creep and oxidation resistance, respectively. The alloy is shown to have attractive combinations of tensile ductility (∼11%), strength (∼800 MPa) and fracture toughness (∼83 MPa$\sqrt{\text{m}}$) in the as-forged condition. However, the tensile and fracture properties are degraded by direct aging in the potential service temperature regime (∼750 °C). The alloy is also shown to have comparable fatigue crack growth resistance to mill annealed Ti-6Al-4V [8], inconnel 718 [9] and pure Nb [10] in the near-threshold regime at 25 and 750 °C. However, the fatigue crack growth rates in the intermetallic alloy are significantly faster in the Paris regime, especially at high stress ratios and elevated-temperature (750 °C).

The paper is divided into seven sections. The materials and microstructures are described in Section 2 before discussing the fracture mechanisms in Section 3. Tensile properties and fracture toughness data are then presented in Sections 3 and 4, respectively. Fatigue crack growth rate data and the micromechanisms of

TABLE I Actual compositions in atomic percent of the Nb-41Ti-11Al-1.5Mo-1.5Cr alloy

Nb	Al	Ti	Mo	Cr	O	N	H	C	Cu
Bal	11.04	41.10	1.5	1.53	0.309	0.033	0.360	0.055	0.042

fatigue crack growth in Section 5. The implications of the current results for potential high temperature structural applications are examined in Section 6 along with recently obtained oxidation data. Salient conclusions arising from this work are then summarized in Section 7. The paper highlights the balance of properties that can be engineered in niobium aluminide intermetallics. However, there is a need for further research and development on this new class of damage tolerant intermetallic materials.

2. Materials

The alloy that was examined in this study was produced by triple vacuum-arc-remelting at Pittsburgh Specialty Materials, Pittsburgh, PA. The actual composition of the alloy, determined by wet chemical analysis, is shown in Table I. The ingot material was upset forged into a billet at the U.S. Bureau of Mines in Albany, OR. After forging, electro-discharge machined specimens were heat treated in evacuated (10^{-4} Pa) quartz capsules at 750 °C for 25 h (direct aged). The direct aging heat treatment (DA) was used to stabilize the microstructure in the potential service temperature regime.

The metallographic specimens were ground and polished to a final mirror finish. Significant efforts were made to obtain a good etch for the intermetallic Nb-11Al-41Ti-1.5Mo-1.5Cr alloy. In the end, a solution of 25% lactic acid, 25% concentrated (30%) hydrogen peroxide, 25% hydrofluoric acid and 25% nitric acid was used to etch the specimens. The etch attacked the direct aged specimens much more aggressively, etching the specimens in 1/20th the time required for the as-forged condition.

The etched specimens had similar average grains sizes (∼55 μm for the direct aged, and ∼52 μm the for the as-forged condition). Figs 1a–c show the microstructures of both specimens. The stabilized microstructure of the direct aged specimens clearly shows a second phase precipitating out near the grain boundaries (Fig. 1c). The matrix material in both the as-forged and directed-aged specimens has a semi-ordered body centered cubic crystal structure. The second phase platelets in the direct-aged matrix have an orthorhombic crystal structure [6].

3. Tensile properties

Duplicate tensile tests were performed on smooth, dog bone shaped specimens that were produced via electro-discharge machining. The specimens had rectangular cross sections, and the gauge dimensions were measured to be $\sim 3 \times 12.7 \times 25.4$ mm. The tensile tests were conducted in accordance with ASTM E-8 specifications [11]. The tensile specimens were loaded continuously to failure at a constant strain rate of $5 \times 10^{-4}\,s^{-1}$. The test results show that Nb-11Al-41Ti-1.5Mo-1.5Cr has an average modulus of ∼810 GPa and a 0.2% offset yield strength ∼788 MPa in the as-forged condition. The equivalent properties for the direct-aged alloy (750 °C/25 h) were ∼974 GPa and ∼995 MPa, respectively.

Stress-strain curves obtained from as-forged and direct-aged (750 °C/25 h) Nb-11Al-41Ti-1.5Mo-1.5Cr are presented in Fig. 2. This alloy exhibits strain softening in the as-forged condition. The as-forged alloy also has a flow strength of ∼788 MPa (Fig. 2). However, it exhibits a significant increase in strength and strain hardening after direct aging at 750 °C which tends to increase the volume fraction of orthorhombic phase. Furthermore, the ductility is degraded from ∼11 to 2.5% after direct aging at 750 °C. Failure of the as-forged specimen occurred predominantly via ductile dimpled fracture (Fig. 3a). The loss of tensile ductility in the direct-aged alloy was associated with a transition from ductile dimpled fracture (in the as-forged condition) to a mixed fracture mode consisting primarily of intergranular facets and some incidence of ductile dimpled fracture.

Since the partially ordered B2 phase is essentially body centered cubic (b.c.c.) in nature, there are numerous possible slip systems that can operate in the alloy. The appearance of "wavy" slip traces on the deformed surfaces of the tensile specimens is a common indication of multislip in b.c.c. materials. Fig. 4 shows a high magnification (SEM) photo of one side of an as forged specimen. Evidence of wavy slip was prevalent across the deformed gauge sections of the as-forged specimens. However, very little evidence of slip was observed on the deformed surfaces of the direct-aged specimens.

The fracture surfaces of both the as forged and direct aged specimens were analyzed via scanning electron microscopy. The mode of failure in the as forged specimens was very different from that of the direct aged material. Ductile dimpled fracture is clearly the dominant mode of failure in the as-forged condition (Fig. 3a). Examination of the fracture surface of the direct aged tensile specimen revealed that the dominant failure mode was cleavage fracture in this condition (Fig. 3b).

4. Fracture toughness

Duplicate fracture toughness tests were conducted on single edge notched (SEN) specimens with dimension of $25.4 \times 25.4 \times 65$ mm. The SEN specimens were precracked under compression fatigue loading [2–4] prior to fracture toughness testing under three-point bending. The fracture toughness tests were conducted in accordance with ASTM E399 specifications [12]. The specimens were loaded continuously to failure at a loading rate corresponding to a stress intensity factor increase rate of ~ 1 MPa $\sqrt{\text{m}} \cdot \text{s}^{-1}$. The failure modes in the specimens were then examined under a scanning electron microscope.

Fracture toughness data obtained from the L-S and L-T orientations are summarized in Table II for

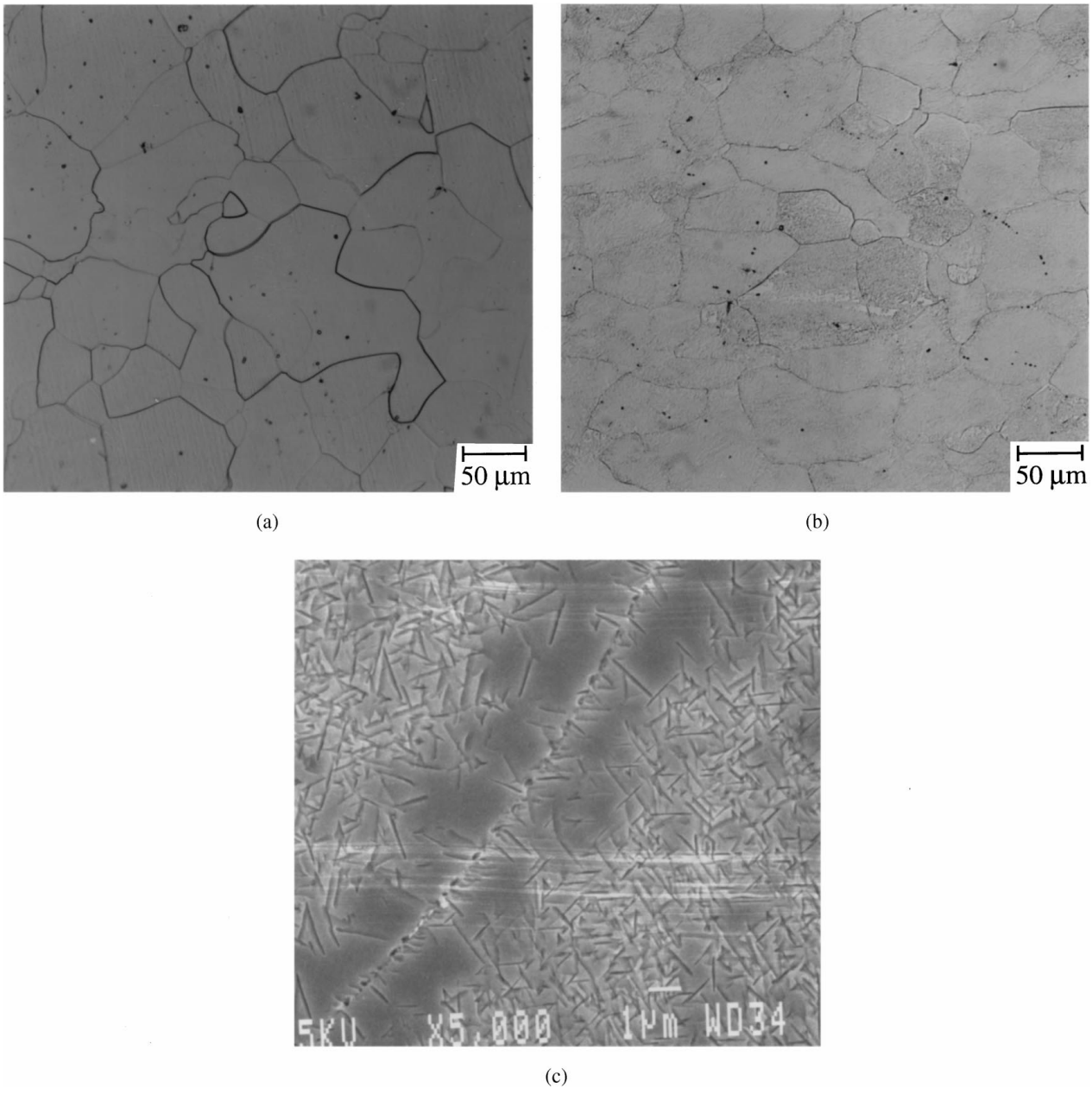

Figure 1 (a) Microstructual profile of the as-forged sample (b) microstructural profile of the sample in the direct-aged condition; and (c) needle-like orthorhombic platelets in a matrix of B2 in the microstructure of the direct aged material. Note the precipitate free zone in the vicinity of the B2 grain boundary.

TABLE II Summary of fracture toughness values obtained in Nb-11Al-41Ti-1.5Mo-1.5Cr alloy

Processing condition	Orientation	Fracture toughness
As-Forged	L-S	83 MPa$\sqrt{m}$
Direct aging	L-S	46 MPa$\sqrt{m}$
Direct aging	L-T	32 MPa$\sqrt{m}$

as-forged and direct-aged alloys. This shows that the fracture toughness levels are somewhat affected by crack orientation (with respect to microstructure) and direct aging. The as-forged alloy has a fracture toughness of ~83 MPa$\sqrt{m}$ in the L-S orientation. This decreased to ~46 MPa$\sqrt{m}$ after direct aging. The fracture toughness level in the L-T orientation also decreased to ~32 MPa$\sqrt{m}$ after direct aging.

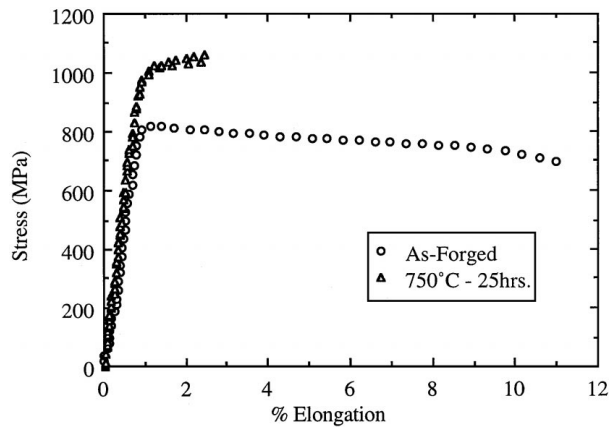

Figure 2 Stress-strain behavior of Nb-11Al-41Ti-1.5Mo-1.5Cr alloys.

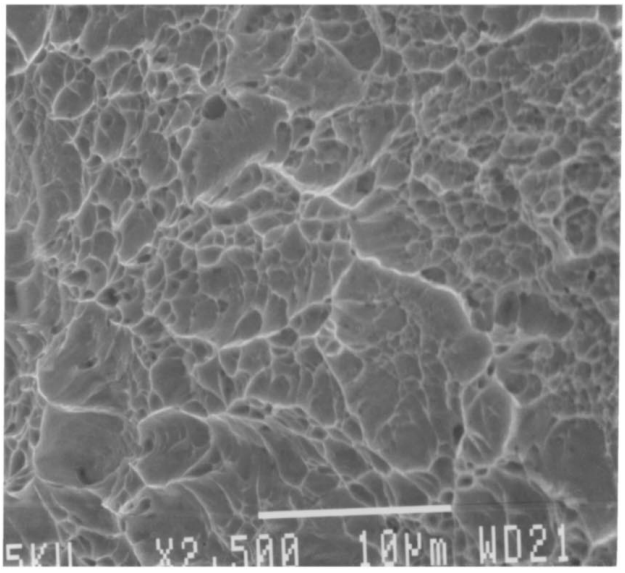

(a)

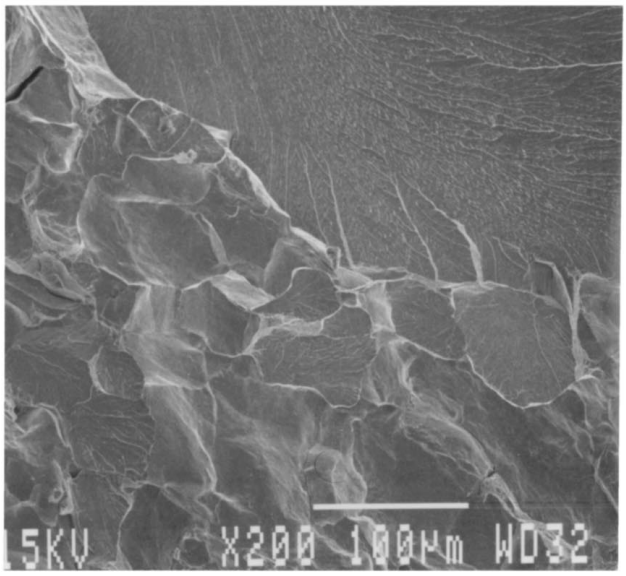

(b)

Figure 3 Scanning electron micrograph of the fractured surface in the Nb-41Ti-11Al-1.5Mo-1.5Cr alloy. (a) As-forged and (b) direct aged (750 °C/25 hrs).

The trends in the fracture toughness data were consistent with the changes in the fracture modes in the fracture modes. Also, the observed changes were similar to those discussed earlier for tensile fracture, i.e. the relatively high fracture toughness levels were associated with ductile dimpled fracture in the as-forged condition, while the lower fracture toughness levels were associated with mixed, predominantly cleavage fracture modes. The reasons for the transition from ductile dimpled fracture to brittle cleavage fracture are unknown at present.

5. Fatigue crack growth

Fatigue crack growth experiments were also conducted on the SEN specimens with the same geometry as the fracture toughness specimens. The fatigue crack growth experiments were carried out in laboratory air (relative humidity approx. 40%) at 25 and 750 °C. All the tests were performed under computer control. The tests at 25 °C were carried out at stress ratios, $R = K_{\min}/K_{\max}$, of 0.1 and 0.5, while the 750 °C were conducted at a stress ratio, $R = K_{\min}/K_{\max}$ of 0.1. Crack growth was monitored using direct current potential drop methods. Crack growth was also monitored with a high resolution ($\sim 1\ \mu$m) Questar telescope connect to a video monitoring unit. The tests were initiated at stress intensity factor ranges of $\sim 12\ \text{MPa}\sqrt{\text{m}}$. Fatigue crack growth rate data were then obtained from load-shedding tests at stress ratios of 0.1 and 0.5. A load-shedding rate, C, of $-0.08\ \text{mm}^{-1}$ was employed initially until near-threshold conditions were reached. A constant load corresponding to stress intensity ranges of $\sim 10\ \text{MPa}\sqrt{\text{m}}$ was then applied to grow the cracks out to failure. Similar experimental methods were used in the room and elevated temperature (25 and 750 °C) fatigue crack growth experiments. However, crack closure was only monitored at room temperature using back face strain gauges [13]. The fatigue fracture modes were examined using scanning electron microscopy.

The room-temperature fatigue crack growth rate data are presented in Fig. 5. The Paris exponents are typically between 2 and 4. Hence, the slopes of the $\text{d}a/\text{d}N - \Delta K$ curves are comparable to those of ductile metals and their alloys. However, the near fatigue crack growth rates at an R of 0.5 were approximately twice as fast as those at R of 0.1. The growth rates at both R-ratios were similar in the Paris regime. However, the growth rates in the high-ΔK regime were much faster at the stress ratio of 0.5.

Fatigue crack growth in all three regimes (low-ΔK, Paris, and high-ΔK) occurred by a "cleavage-like" fracture mode in the direct aged condition (Fig. 6). However, a higher incidence of secondary cracking was observed with increasing in the high-ΔK regime. Furthermore, the incidence of secondary cracking also appeared to increase with increasing-ΔK, especially in the high ΔK regime. The increase in the incidence of secondary cracking was also found to be greater at the higher stress ratio, R, of 0.5. No evidence of crack closure was detected by compliance (notch-mouth clip gauge) techniques at room temperature (25 °C).

The fatigue crack growth rates obtained at 750 °C were close to those obtained at 25 °C at a stress ratio of 0.1. A "cleavage-like" fracture mode was also observed at 25 and 750 °C in the near-threshold, Paris and high ΔK regimes (Fig. 7). Furthermore, it is important to note here that thermally-induced oxides were not observed on the fracture surfaces of the specimens that were tested at 750 °C. This suggests that oxide-induced crack closure does not play a significant role in the fatigue crack growth behavior at 750 °C. This is in contrast with non-chromium containing niobium aluminide alloys (Nb-15Al-40Ti and Nb-12.5Al-44Ti-1.5Mo) in which thermally-induced oxide layers (with thicknesses comparable to the crack opening displacements) were formed during fatigue crack growth testing at 750 °C [2, 5]. The thermally-induced oxide layers are clearly sufficient to cause oxide-induced crack closure (which decrease the elevated-temperature fatigue crack growth rates) in non-chromium containing niobium aluminide alloys.

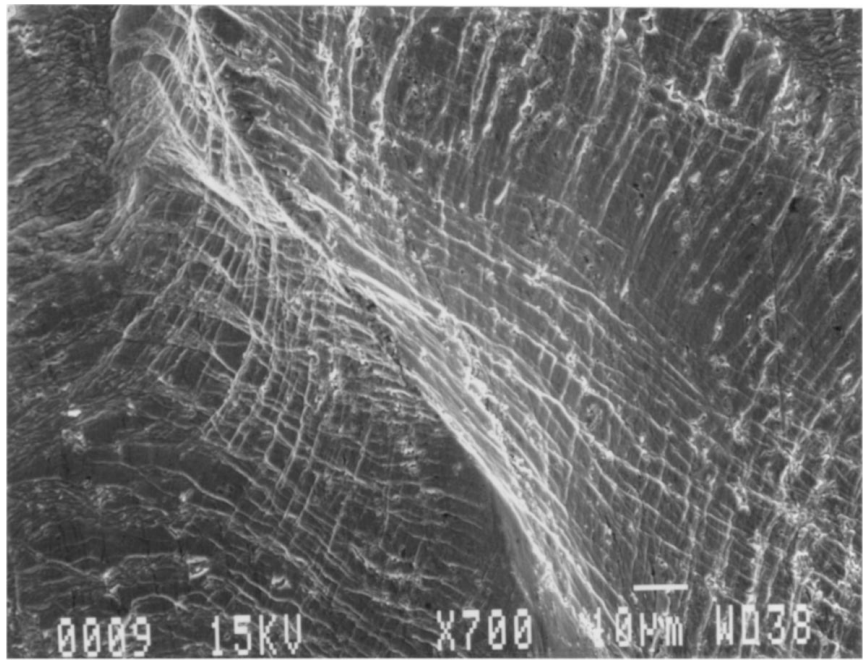

Figure 4 Wavy slip traces marking the surface of the AF samples that formed during tensile.

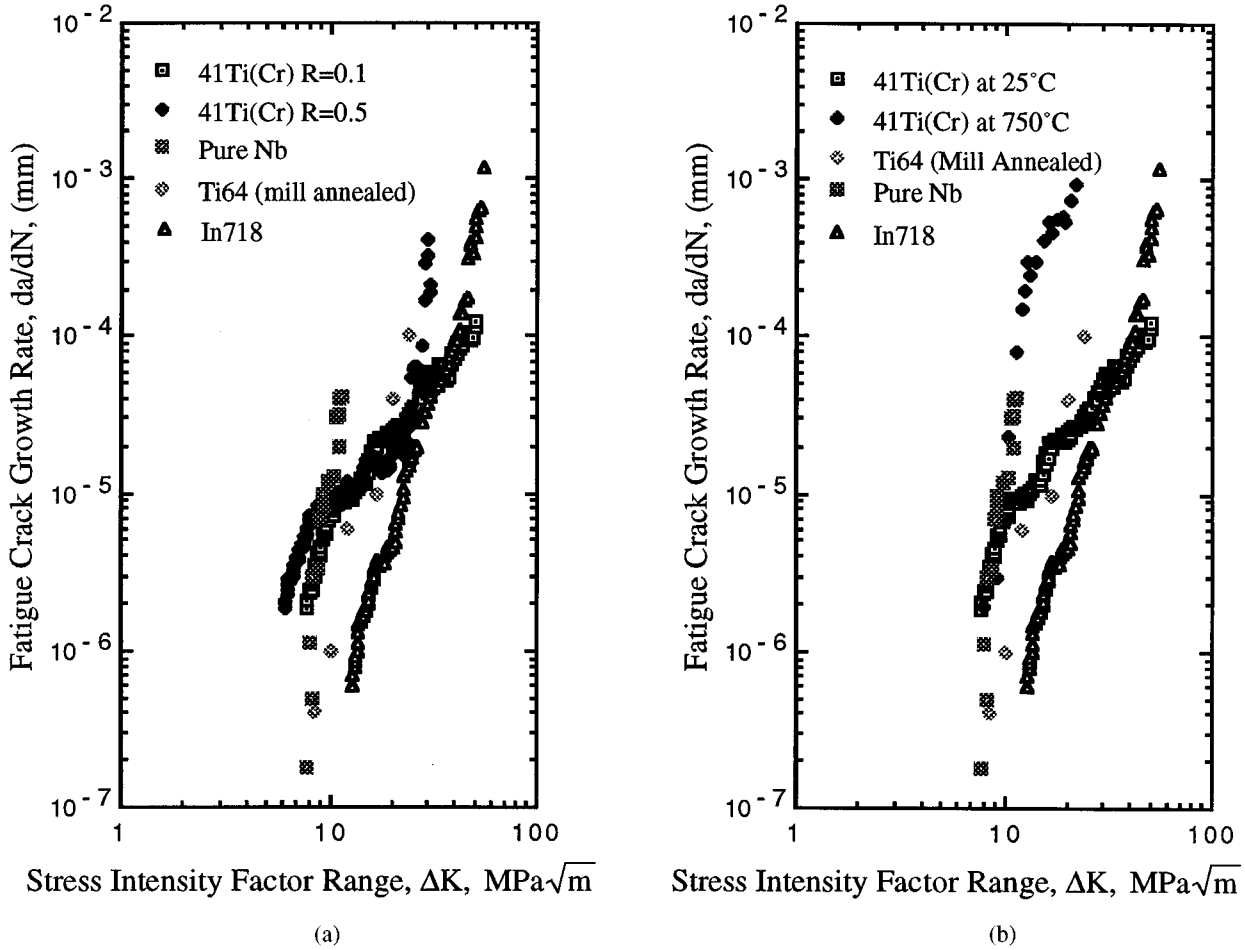

Figure 5 Summary of fatigue crack rate for Nb-11Al-41Ti-1.5Mo-1.5Cr alloys (Ti-64 data taken from Ref. [8], in 718 data taken from Ref. [9] and Nb data from Ref. [10]).

6. Implications

The above results are significant because of the balance of properties of the Nb-11Al-41Ti-1.5Mo-1.5Cr alloy (Table II and Figs 2 and 5). Unlike most niobium-base intermetallic systems, which typically have low room-temperature fracture toughness levels of ~10–40 MPa$\sqrt{m}$ (Fig. 8) [14–24], the current alloy has fracture toughness levels of ~32–83 MPa$\sqrt{m}$,

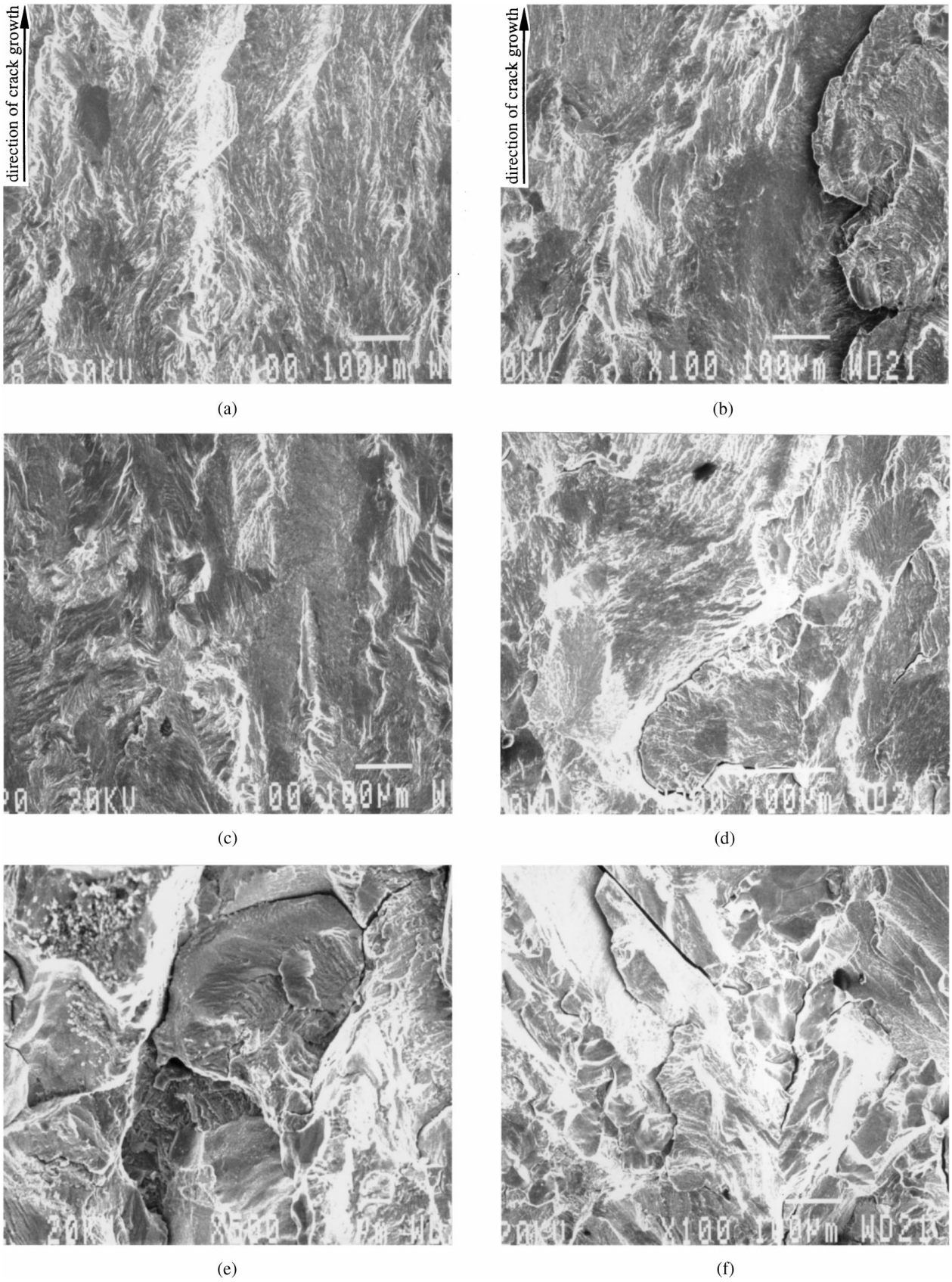

Figure 6 Typical fatigue fracture observed at room-temperature. (a, b) low (c, d) mid (e, f) high ΔK regimes. (R= 0.1 for a, c and e, R = 0.5 for b, d and f).

depending on the processing/heat treatment conditions. The high fracture toughness levels in the multicomponent alloy (Nb-11Al-41Ti-1.5Mo-1.5Cr) are greater than those of niobium-base *in-situ* composites (Nb-10Si, Nb-Cr-Ti and Nb-Cr-Hf-Ti-Si), and comparable to those of Nb-13Cr-37Ti and Nb-15Al-40Ti. Similar fracture and fatigue resistance has been reported by Loria [24] for a multicomponent body centered cubic Nb-35Ti-6Al-5Cr-8V-1W-0.5Mo-0.5Hf alloy.

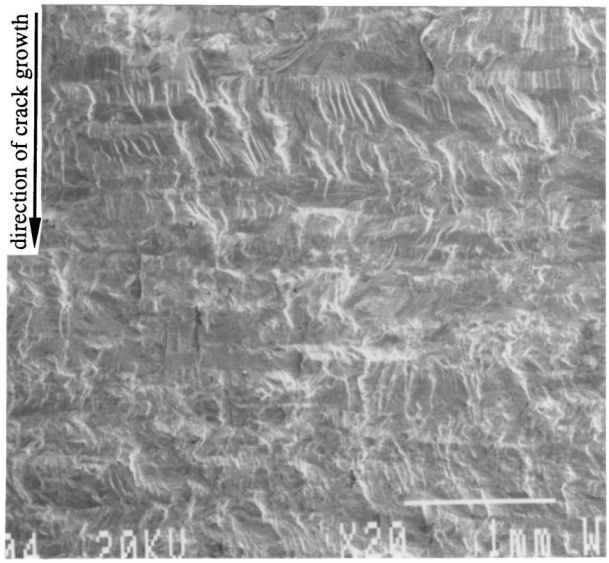

(a)

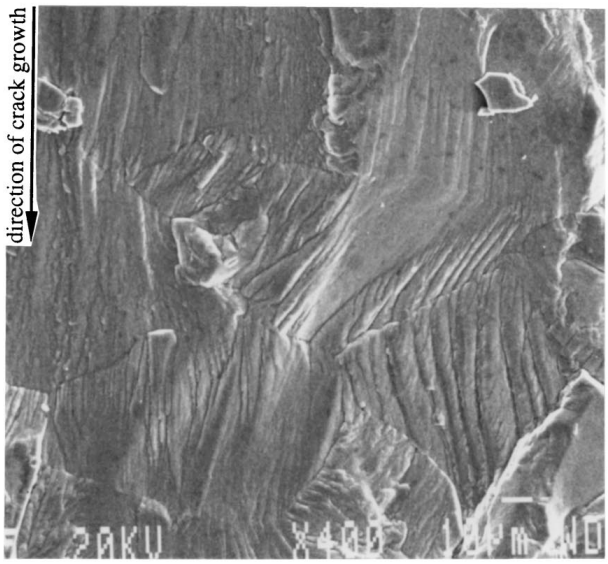

(b)

Figure 7 Typical fatigue fracture modes observed at 750 °C.

Nevertheless, the wide range of fracture toughness data obtained for the multicomponent Nb-11Al-41Ti-1.5Mo-1.5Cr alloy are still of some concern since they indicate a degradation in fracture toughness with increasing thermal exposure in the potential service temperature regime of ∼750 °C (Table II). Further aging studies are therefore needed to investigate the effects of long term aging on microstructural stability and fracture properties before the multicomponent Nb-11Al-4lTi-1.5Mo-1.5Cr alloy can be fully considered for high temperature structural applications.

In any case, the balance of room-temperature fracture toughness (Table II), tensile properties (Fig. 2), and room- and elevated-temperature fatigue crack growth resistance (Fig. 5) of the multicomponent Nb-11Al-41Ti-1.5Mo-1.5Cr alloy is encouraging. Furthermore, the multicomponent alloy has been shown to have better isothermal and cyclic oxidation resistance than non-chromium containing niobium aluminide alloys [6]. This is shown in Fig. 9a–c using isothermal oxidation data, which is taken from Ref. [6] for a range of niobium aluminide based intermetallics at temperatures between 650 and 850 °C. Alloying with chromium consistently reduces the isothermal oxidation rates in this temperature regime. The Cr-containing alloys exhibit the slowest oxidation rates when compared to all of the other niobium aluminide alloys in this figure. Also, the multicomponent Nb-11Al-41Ti-1.5Mo-1.5Cr alloy consistently exhibits the best isothermal oxidation resistance at temperatures between 650 and 850 °C.

Further evidence of the potential of the current alloy for elevated-temperature structural applications is presented in Fig. 5. This shows that the multicomponent alloy exhibits relatively slow fatigue crack growth rates in the near-threshold regime. However, the fatigue crack growth rates in the Paris regime are relatively fast at 750 °C, compared to those in pure Nb and Ti-6Al-4V at room-temperature. Fatigue design at elevated-temperature may, therefore, be limited to the near-threshold or short crack regimes.

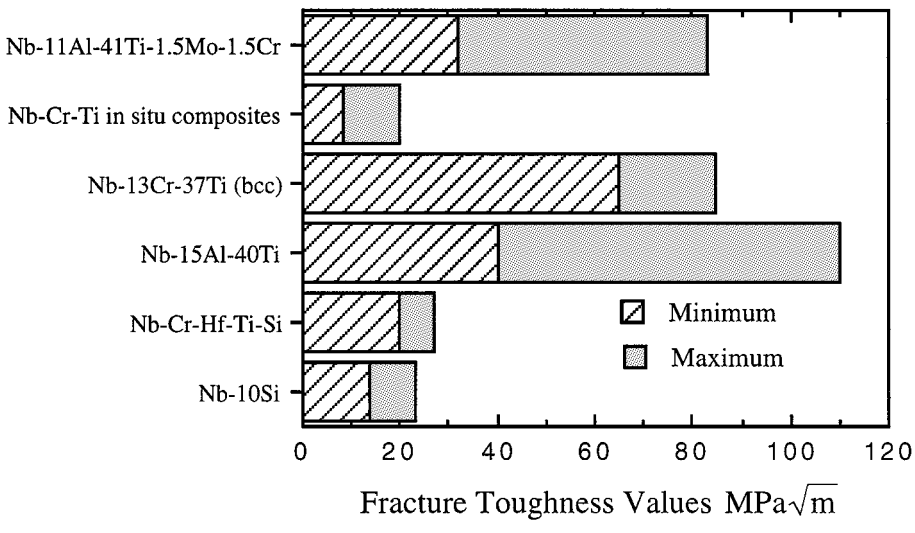

Figure 8 Comparison of fracture toughness values with those of other niobium base intermetallics.

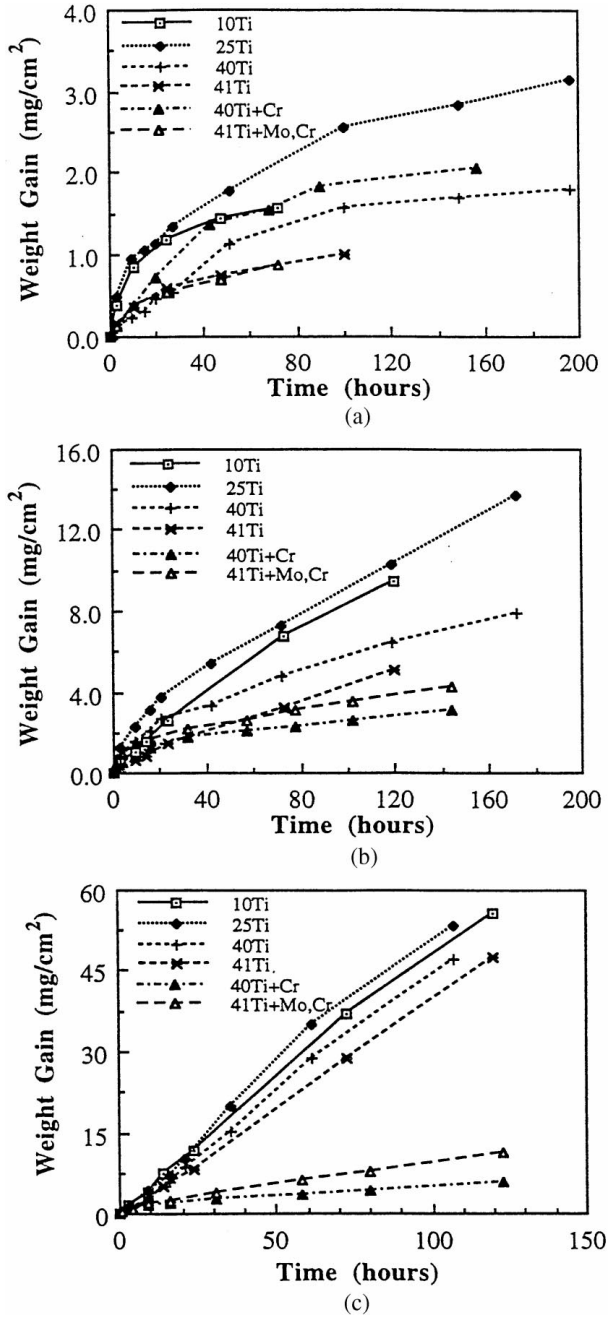

Figure 9 Effects of alloying on isothermal oxidation kinetics at: (a) 650 °C; (b) 750 °C and (c) 850 °C (10Ti = Nb-15Al-10Ti; 25Ti = Nb-15Al-25Ti; 40Ti = Nb-15Al-40Ti; 41Ti = Nb-12.5Al-41Ti-1.5Mo; 40Ti + Cr = Nb-15Al-40Ti-1.5Cr, and 41Ti + Cr = Nb-11Al-41Ti-1.5Mo-1.5Cr).

Assuming that potential applications may involve the application of stresses that are approximately equal to half of the 0.2% offset yield strength, it is possible to estimate a critical crack length for a fatigue threshold based design. For a 0.2% offset yield strength, σ_{ys}, of 995 MPa and a fatigue threshold, ΔK_{th}, of approx. 6.5 MPa$\sqrt{m}$ in the direct aged condition, an estimate of the critical crack length, a_c, may be obtained from [25]:

$$a_c = \frac{1}{\pi}\left[\frac{2\Delta K_{th}}{\sigma_{ys}}\right]^2 \quad (1)$$

Substituting the above values into Equation 1 gives a critical value of crack length to be approx. 54 μm. This is clearly in the short crack regime where the crack lengths are comparable to the grain sizes (Fig. 1a–c). It is, therefore, important to conduct further research on the fatigue crack growth of microstructurally short cracks in the current multicomponent alloy.

It is clear from the current study that the multicomponent Nb-11Al-41Ti-1.5Mo-1.5Cr alloy exhibits a balance of fatigue and fracture resistance, tensile ductility and oxidation resistance that is clearly remarkable. The balance of properties have led some aeroengine companies to explore potential applications for niobium aluminide based alloys in nozzles and blades in gas turbines. However, further alloy development and heat treatment studies are needed to optimize these alloys for such applications. Detailed studies of fatigue crack initiation and possible short crack anomalies are also needed before the alloys can be fully considered for service in gas turbines.

7. Summary

(1) The room temperature ductility of the Nb-11Al-41Ti-1.5Mo-1.5Cr alloy is ~11.5% in the as-forged condition. However, direct aging at 750 °C for 25 h degrades the tensile ductility to ~2.5% at room temperature. The degradation in the tensile ductility is associated with a transition from ductile dimpled fracture mode to a cleavage fracture mode. Direct aging also results in the precipitation of orthorhombic platelets and significant strengthening at room temperature.

(2) The fracture toughness of the Nb-11Al-41Ti-1.5Mo-1.5Cr alloy is ~80–85 MPa$\sqrt{m}$ in the as-forged condition. Such high fracture toughness levels are comparable to values reported for ductile metals and their alloys. However, the fracture toughness is somewhat degraded after direct aging at 750 °C. Some orientation dependence of fracture toughness is also observed, with the L-S orientation having a higher fracture toughness than the L-T orientation in the direct aged condition.

(3) The room temperature fatigue crack growth rates in the near-threshold and high ΔK regimes at a stress ratio of 0.5 are twice that at a stress ratio of 0.1. The near-threshold fatigue crack growth rates are similar at 25 and 750 °C at a stress ratio of 0.1. However, the fatigue crack growth rates in the Paris regime are much higher at 750 °C at a stress ratio of 0.1.

(4) Fatigue crack growth at room temperature occurs by a cleavage-like fracture mode in the near threshold, Paris and high ΔK regimes. Similar fatigue fracture modes are observed at 25 and 750 °C in the three regimes of crack growth. However, some incidence of secondary cracking which appears to increase with increasing ΔK and increasing stress ratio.

(5) The multicomponent niobium aluminide alloy examined in this study exhibits a balance of properties (tensile ductility, fracture toughness, fatigue resistance and oxidation resistance) that indicates the potential for structural applications in the temperature regime below 800 °C.

Acknowledgements

The research was initiated with the support of a grant from The Office of Naval Research, with Dr. George Yoder as Program Monitor. It was completed with the

support of the Division of Material Research of The National Science Foundation, with Dr. Bruce MacDonald as Program Monitor. The authors are grateful to Dr. Craig Wocjik for assistance with the multi-step forging process at the U.S. Bureau of Mines.

References

1. D. H. HOU, J. SHYUE, S. S. YANG and H. L. FRASER, in "Alloy Modeling and Design," edited by G. M. Stocks and P. Z. A. Turch (TMS, Warrendale, PA, 1994) pp. 291–298.
2. F. YE, C. MERCER and W. O. SOBOYEJO, *Metall. Mater. Trans.* (1998) pp. 2361–2374.
3. J. D. PASQUALE, D. GAHUTU, D. KONITZER and W. O. SOBOYEJO, in "High Temperature Ordered Intermetallic Materials VI," edited by J. A. Horton, S. Hanada, I. Baker, R. D. Noebe and D. S. Schwartz (Materials Research Society, Pittsburgh, PA, 1994) pp. 1347–1352.
4. W. O. SOBOYEJO, J. DiPASQUALE, F. YE and T. S. SRIVATSAN, *Metall. Mater. Trans.* (1998), in press.
5. T. S. SRIVATSAN, C. DANIELS, S. SRIRAM, K. P. DHANA SINGH, D. KONITZER and W. O. SOBOYEJO, in Proceeding of the Symposium on Fatigue and Fracture of Ordered Intermetallics II, edited by W. O. Soboyejo, T. S. Srivatsan and R. O. Ritchie (TMS, Warrendale, PA, 1995) pp. 287–308.
6. Y. LI, W. O. SOBOYEJO and R. A. RAPP, *Metall. Trans.* (1998), in press.
7. B. V. COCKERMAN, H. J. SCHMUTZLER, J. SHYUE, K. HOSHINO, S. MENG, R. WHEELER and H. L. FRASER, Materials Research Society, Pittsburgh, PA, 1994, pp. 1327–1332.
8. S. DUBEY and A. B. O. SOBOYEJO, *Acta Metall. Mater.* **45** (1997) 2777–2787.
9. C. MERCER and W. O. SOBOYEJO, in "Superalloy 718, 625, 706 and Various Derivatives," edited by E. A. Loria, 1997, pp. 577–586.
10. N. POLVANICH and K. SALAMA, in "ASTM STP 962," edited by L. Raymond, 1987, pp. 417–427.
11. Annual Book of ASTM Standards (American Society for Testing and Materials, Philadelphia, Pennsylvania, E-8 Code, 1993) Vol. 03.01, pp. 679–706.
12. Annual Book of ASTM Standards (American Society for Testing and Materials, Philadelphia, Pennsylvania, E-399 Code, 1993) Vol. 03.01, pp. 509–539.
13. W. O. SOBOYEJO and J. F. KNOTT, *International Journal of Fatigue* **12** 403–407.
14. J. D. RIGNEY and J. J. LEWANDOWSKI, *Metall. Mater. Trans.* **27A** (1996) 3292–3306.
15. P. R. SUBRAMANIAN, M. G. MENDIRATTA and D. M. DIMIDUK, *Journal of Metals*, January (1996) 33–38.
16. B. P. BEWLAY, J. J. LEWANDOWKSI and M. R. JACKSON, *ibid.*, August (1997) 44–67.
17. B. P. BEWALY, M. R. JACKSON and H. A. LIPSITT, *Metall. Mater. Trans.* **27A** (1996) 3801–3808.
18. D. L. DAVIDSON, K. S. CHAN and D. L. ANTON, *Metall. Mater. Trans A* **27A** (1996) 3007–3018.
19. *Idem.*, *ibid.* **28A** (1997) 1797–1808.
20. K. S. CHAN, *Metall. Mater. Trans.* **23A** (1992) 183–99.
21. D. BLOYER, K. T VENKATESWARA RAO and R. O. RITCHIE, *Mater. Sci. Eng.* **A239–A240**, 393–398.
22. K. BADRINARAYANAN, A. L. McKELVEY, K. T. VENKATESWARA RAO and R. O. RITCHIE, *Metall. Mater. Trans.* **27A** (1996) 3781–3792.
23. D. R. BLOYER, K. T. VENKATESWARA RAO and R. O. RITCHIE, Layered Materials For Structural Applications, Materials Research Society, J. Lewandowski, C. H. Ward, M. R. Jackson and W. H. Hunt, Jr., Materials Research Society, Pittsburgh, PA, Vol. 434, 1996, p. 43.
24. E. A. LORIA, *Mater. Sci. Eng.* **A254** (1998) 63–66.
25. F. McCLINTOCK, in the Proceedings of the Symposium on High-Cycle Fatigue: the Paul Paris Symposium, edited by W. O. Soboyejo and T. S. Srivatsan (TMS, Warrendale, PA, 1997) pp. 1–24.

Received 5 January
and accepted 9 February 1999